

## FINITE ELEMENT MODELS FOR THE COMPUTATION OF THE TRANSIENT POTENTIAL AND FIELD DISTRIBUTION IN THE WINDING SYSTEM OF HIGH VOLTAGE POWER TRANSFORMERS

Amir M. MIRI    Norbert A. RIEGEL    Andreas KÜHNER

Universität Karlsruhe, IEH, Kaiserstrasse 12, 76128 Karlsruhe, Germany  
phone: ++49 721 608 3061, fax: ++49 721 695224, email: miri@ieh.ctec.uni-karlsruhe.de

### Abstract:

The knowledge of the potential and field distribution in the winding system of a transformer, during transient excitation is vital to its construction. In this paper the problem of modeling large numbers of winding turns is solved with detailed finite element models. Frequency-dependent phenomena such as skin and proximity effects in the conductors, tan $\delta$  losses in the insulation, or the displacement of the magnetic flux in the iron core are considered. The two methods are applied to investigate the transient behavior of a 66 kV distribution transformer and a 420 kV generator transformer using both direct transient analysis and with ac analysis and the application of the FFT. The computed results are compared with measurements to verify the developed methods. Ac analyses are performed to obtain the frequencies at which the winding system is most endangered.

**Key words:** ISH, Transients, Transformer

### 1. Introduction

Transformers in operation are subject to various kinds of high voltage stresses, caused by lightning strikes, disconnecting operations or system disturbances. The rise times of the initiated travelling waves are in the range of ms to ns and correspond to frequencies in the range of kHz to several MHz. If the dominating frequency of a voltage surge corresponds to one of the natural frequencies of the winding system, resonance excitations are caused. These cause high voltage stresses in parts of the winding system, which can lead to insulation faults such as interturn faults, flashovers and short circuits. Since measurements can only be carried out at specific places in the winding system, e.g. at the transformer's regulation taps, numerical simulation is the only way to determine the high frequency performance of a transformer. /1/

To take into account the skin effect, proximity effect and the displacement of the magnetic flux within the transformer core, several results obtained by FEM calculations can be used. Alternatively results yielded by network calculations can be used in the transformer's FEM model.

As a result of the transformer's non-linear and frequency-dependent parameters, the calculation of the transient and resonant behavior of a transformer leads to a non-linear field problem. Due to the saturation of the transformer core and hysteresis, core losses and non-linear inductances occur. Fur-

thermore, eddy current effects lead to frequency-dependent parameters.

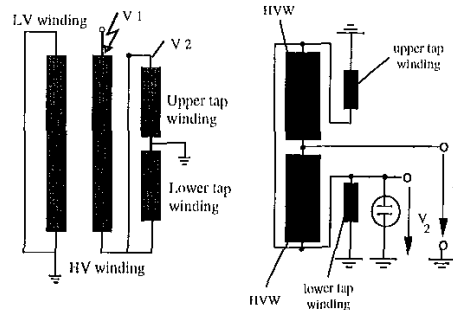


Fig. 1: Test arrangement for the 66 kV distribution transformer (left) and for the 420 kV generator transformer (right)

Due to the transient processes within the winding system the current density is non-uniformly distributed across the conductor's cross section, leading to a considerable increase of the damping if the skin depth reaches the conductor's dimensions. These losses are a result of the skin effect (the influence of the conductor's self-field on itself) and the proximity effect (the influence of the magnetic field of nearby conductors). The skin and proximity effect losses can be calculated separately and superposed.

### 2. Calculation of the Skin and Proximity Effect Losses in the Conductors

The analytical calculation of skin effect losses can only be performed for simple arrangements. Hence, numerical methods have to be used to determine the current distribution across the conductor's cross section and the frequency dependent losses /2/.

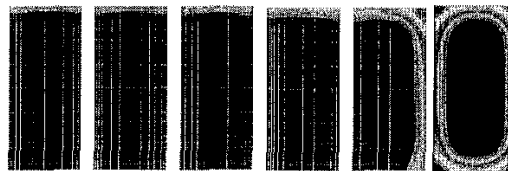


Fig. 2 : Proximity (left) and skin (right) effect, 5 kHz

Especially the core and the conductors have to be simulated by separate models. The obtained characteristics are then combined in a three dimensional three-phase model of the 66 kV distribution transfor-

mer. A similar analysis is performed for the 420 kV generator transformer.

The eddy current distribution of the conductor is shown in Fig.2 for 5 kHz. The displacement of the current density can easily be recognized.

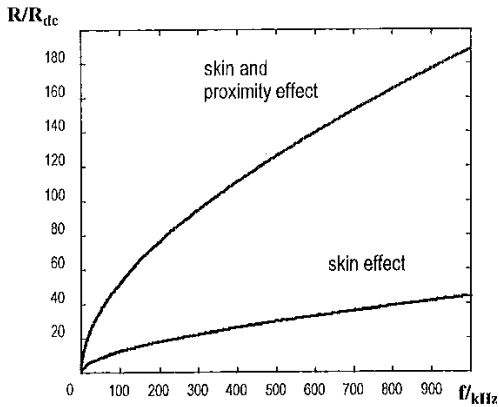


Fig. 3 : Resistance of a disc unit in the H. V. winding

**3. FEM Model of the Core**

In order to simulate the displacement of the magnetic flux in the transformer core a two dimensional model is developed [4].

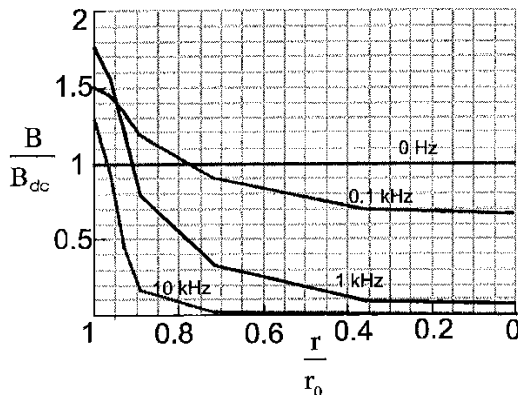


Fig. 4 : Magnetic flux in the core at different frequencies

If a transformer core consists of steel layers with thickness  $h$ , conductivity  $\sigma$  and permeability  $\mu$ , the damping and the inductivity change with increasing frequency :

$$R \approx L_{DC} \cdot \frac{1}{h} \sqrt{\frac{2\omega}{\sigma\mu}} \quad L \approx L_{DC} \cdot \frac{1}{h} \sqrt{\frac{2}{\omega\sigma\mu}} \quad (5)$$

Since the transformer core consists of laminated steel, the conductivity in the model is reduced in the horizontal direction in such a way that the same changes in damping and inductivity are obtained [3]. Fig.4 shows the flux as a function of the core radius. At 10 kHz the magnetic flux within the transformer core is almost completely displaced out of the core,

which confirms the approach used in calculating the network inductances, where transformer coils were regarded as air-core reactors.

**3. FEM Model of the Transformer**

Based on the given geometrical data a complete three-phase model of the 66 kV distribution transformer is developed. Since it is impossible to model each turn, because of the outrunning number of elements, the equivalent material method has to be used [3].

The basic idea is to increase the relative permeability constant and the relative dielectricity constant by the same ratio by which the number of winding turns is reduced. As a result, the propagation velocity is reduced and the travelling time is kept constant as well as the reflection factors.

First, a single phase of the transformer is modelled to compare the calculated results to available measurements. The transformer core is modelled using penta elements with anisotropic conductivity considering the influence of the laminated steel. The low voltage winding is reproduced by a conductive cylinder consisting of quad elements.

Calculations have shown that the influence of the low-voltage winding on the potential distribution inside the transformer is negligible because it is grounded under test conditions. As a result, the number of elements can be reduced remarkably by leaving it out. By using the equivalent material method the number of turns of the high voltage winding is reduced from 553 to 26. Each turn consists of 12 quad elements so that they occupy the same space as the original winding. The distance between two layers of quad elements is greater than the distance between two discs of the actual high voltage winding. For unchanged capacitances the relative dielectricity constant of the insulating elements is increased. The coarse-step and the fine-step tap windings are modelled by 12 line elements for each turn. Their number of turns is reduced by the same ratio as used for the high voltage winding. The low-voltage, high-voltage and tap windings are separated from each other by many layers of different insulating materials, such as oil, paper or transformer board. The winding of the single phase model is shown in Fig.5.

Based on this single-phase model a three-phase transformer model is developed. It consists of 10445 elements and 8681 grids and is depicted in Fig.6 without its air envelope. At the boundary of the air envelope the time-integrated scalar potential as well as the magnetic vector potential are set to zero.

As an ac analysis of the complete transformer model shows, the first maximum at the connection of the high-voltage winding and tap winding occurs at 72 kHz. Superposing the results of the skin and proximity effect calculations shows that the resistivity of the conductor at this frequency is about 500 times higher than the dc value. Hence, the conductivity of the elements representing the conductors is reduced by this factor for direct transient analysis.

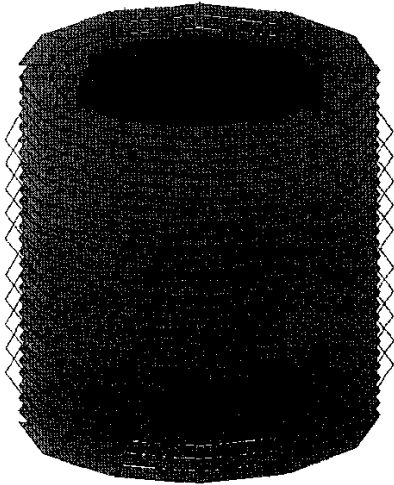


Fig. 5 : Single-phase FEM model of the winding

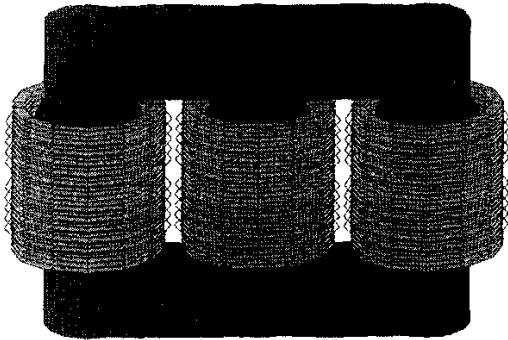


Fig. 6 : Three-phase FEM model of the transformer winding and core

A great disadvantage of solution sequences operating in the time domain is that it is impossible to take into account the frequency dependent material parameters of the transformer conductors and insulation. In order to model frequency dependent materials, ac analyses have to be performed. In addition to the changes of the magnetic flux distribution in the iron core and to the resistivity and inductance of the windings, a frequency dependence of the losses in the insulating materials due to a frequency dependent  $\tan\delta$  can be used. The excitation has to be transformed into the frequency domain using the Fast Fourier Transform (FFT). After the multiplication of the transfer function, obtained by the ac analysis, and the FFT of the excitation function, the inverse FFT (IFFT) can be employed to transform the product to the time domain leading to the desired voltage distribution. In principle the FE method can be used for the whole frequency range, but is restricted by the number of elements.

#### 4. Calculated and Measured Results

Fig.7a and 7b show the results obtained by measurement and calculation. As excitation a 1.2/50  $\mu\text{s}$  lightning impulse test voltage is used.

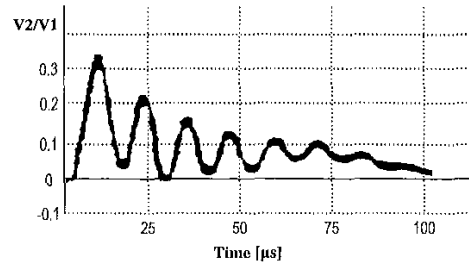


Fig 7a : Measurement results

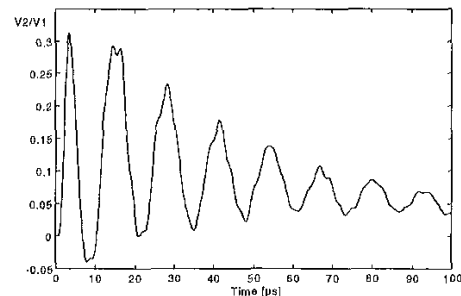


Fig 7b : Finite element analysis direct transient results

Although the results obtained with direct transient analysis show good agreement with the measured values, a method to directly consider the frequency dependence of the material parameters was developed. The material parameters of the transformer are evaluated in the frequency range of interest, which is up to 500 kHz, and ac analyses of the transformer model with modified material parameters are performed in this frequency range. At frequencies close to resonant frequencies the ac analysis is refined. Figure 8 shows the potential distribution of the H.V. winding depending on frequency and location, where  $x/l=1$  refers to the connection of the H.V. winding to the tap winding. The first maximum of the potential at the intersection of both windings occurs at a frequency of 72 kHz.

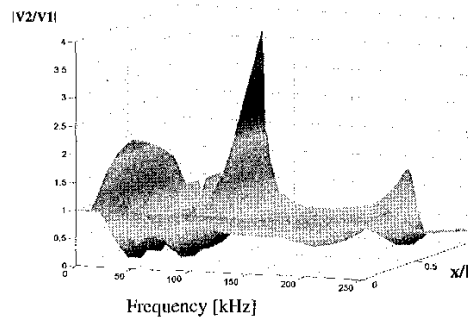


Fig. 8 : Potential distribution in the H.V. winding

At those frequencies where no ac analysis was performed, an interpolating algorithm is used to evaluate the transfer function at equally spaced frequencies. The advantage of this method compared to

direct transient analysis is that for each transformer a time and hardware intensive finite element analysis does not need to be performed for each excitation. If the relative permittivity of the insulating material is set to be complex, the imaginary part represents a frequency dependent conductivity. The frequency range up to 250 kHz is sufficient for excitations with rise times in the range of microseconds. Exceeding the frequency range to 2 MHz does not increase the accuracy. Excitations with smaller rise times require a higher frequency range for the ac analysis.

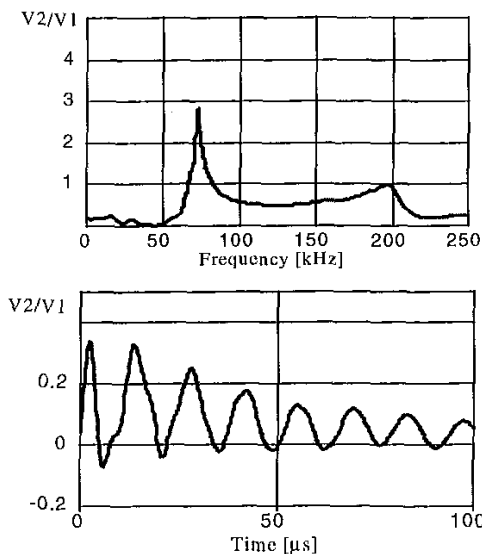


Figure 9: Transient behaviour of a 66 kV distribution transformer calculated with ac analysis (transfer function) with modified material parameters (above), FFT of the excitation and inverse FFT to obtain the transient potential distribution (below).

### 5. Calculation Results and Measurements at the 420 kV Generator Transformer

Each phase of the 420 kV generator consists of a low-voltage winding, a high-voltage winding and a regulating winding.

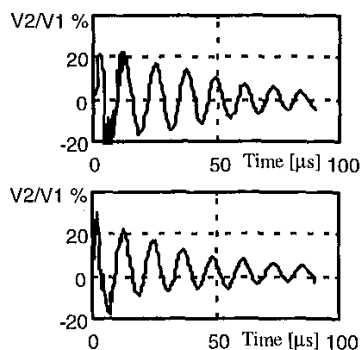


Figure 11: Measurement (above) and calculation results (below)

The high-voltage windings and the regulating windings are performed as disc windings and are divided into two symmetrical parts with opposite winding directions connected in parallel.

Each regulating winding consists of 42 winding turns subdivided into 18 discs, while each high-voltage winding consists of 575 winding turns subdivided into 42 discs. The main frequency of oscillation at the intersection of high-voltage winding and tap winding is 80 kHz.

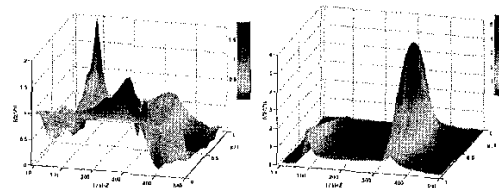


Figure 11: Potential distribution of the high voltage winding (left) and the tap winding (right)

### 6. Conclusion

This paper describes detailed finite element models of a 66 kV and a 36/420 kV power transformer which have been developed using geometrical data. These models allow the investigation of transients inside the transformer disc windings and consider eddy current losses of the windings and the iron core as well as frequency dependent insulation losses. The developed procedure for reducing the number of winding turns in order to limit calculation time and storage requirements leads to accuracy in the calculation. The analysis results are compared to measurement results. An ac analysis is performed to find the location and frequency at which the winding system is most endangered.

### References

- 1 Miri, A.M., Nothaft, M.A., Braess, P. : *Methods for Considering the Eddy Current Losses in the Detailed Model of a HV-Transformer*. In: Proceedings International Conference on Power System Transients, Lisbon Sept. 1995
- 2 Semlyen, A., De Leon, F. : *Time Domain Modelling of Eddy Current Effects for Transformer Transients*. In: IEEE Transactions on Power Delivery, Vol.8, No.1, January 1993
- 3 Miri, A.M., Riegel, N.: *FE Method for the Calculation of the transient Potential Distribution within the Winding System of a Three Phase High-Voltage Transformer*. In: Proceedings MSC Electromagnetics European Users' Conference, Munich 1995
- 4 Miri, A.M., Riegel, N., Huber, S., Marinescu, A. : *Modelling of the Transient Behaviour of High Voltage 3-Phase Power Transformers with Different Regulating Winding Types*. In: International Conference for Electrical Transformers, Bucharest May 1996